

# Influence of yttrium and gadolinium additions on thermal and structural behavior of Cu-Zr bulk metallic glasses

I. V. STASI<sup>a,b\*</sup>, G. NEDELICU<sup>a</sup>, C. GHEORGHIŞ<sup>a</sup>, N. MATTERN<sup>b</sup>, J. ECKERT<sup>b</sup>

<sup>a</sup>Faculty of Mechanic, Dunarea de Jos University, Galați, R-800008, Romania

<sup>b</sup>Leibniz Institute for Solid State and Materials Research Dresden, Helmholtzstrasse 20, Dresden, D-01069, Germany

Interest in finding binary alloys that can form bulk metallic glasses (BMGs) has stimulated recent work on the Cu-Zr system, which is known to show glass formation over a wide composition range. The thermal and structural behaviour of rapidly quenched Cu-Zr alloys were analyzed. The ribbons of  $\text{Cu}_{50}\text{Zr}_{50-x}\text{Me}_x$  (Me=Y,Gd;  $x=5,10,15,20,25$ ) were produced by Melt Spinning method and investigated by using X-ray diffraction, differential scanning calorimetry, scanning electron microscopy and transmission electron microscopy techniques. The characterization of Cu-Zr alloys using DSC related that the reforming activity was strongly correlated with the endothermic heat during the glass state of alloys. Furthermore, the Y or Gd content in Cu-Zr alloys affected the endothermic heat. DSC analyses have confirmed the existence of glass transition, followed by supercooled liquid region in all the composition, in one or two steps. X-ray diffraction patterns of the ribbons before DSC showed that some are amorphous and other partial amorphous. X-ray diffraction patterns recorded for the ribbons heated up to 973 K in DSC using a rate of  $20 \text{ K min}^{-1}$  under a flow of purified argon showed that the samples crystallized. SEM and TEM demonstrated that the microstructural evolution depends on the amount of Y or Gd. The precipitating phases were determined by SEM, TEM and XRD. Finally, crystallization processes of the samples were summarized. In the future the study will be focus to interpret all obtained dates. Therefore, these types of BMGs are very promising for the further development of Cu-Zr-based alloys as engineering materials.

(Received September 1, 2008; accepted October 30, 2008)

**Keywords:** Bulk metallic glasses, Cu-Zr alloys, Y,Gd addition, XRD, DSC, TEM, SEM

## 1. Introduction

Bulk metallic glasses (BMGs) have been largely investigated since the early 1990s due to their unique physical, chemical and mechanical properties being of special interest for a wide range of potential applications.

The precipitation of nanoscale crystalline phases may be used to improve the mechanical behaviour of BMGs. The precipitation of nanocrystals in the amorphous matrix may be induced by addition of elements which can cause partial crystallization during casting or by primary crystallization during heat treatment of the BMG.

Recently, several metallic alloys with high glass forming ability (GFA) were reported and extensive studies had been made in these glasses, such as Zr-Cu-Al [1-4], Zr-Cu-Al-Ni [5-8] and Zr-Cu-Al-Ni-M [9-13] alloys. Very low critical cooling rates are required for these alloys to form metallic glasses, showing the possibility of producing bulk amorphous alloys by conventional casting processes. Without the limitation of size and shape, the amorphous alloys can be widely used as advanced materials.

In comparison with above-mentioned alloy systems, Cu-Zr binary alloys have a relatively low GFA and a narrow supercooled liquid region. However, all above-stated bulk amorphous alloys are based on Cu-Zr binary alloy, which has a higher GFA among binary alloys compared with many other binary ones. It is necessary to study amorphous Cu-Zr alloy, especially its crystallization behaviour, which can be a contribution to understanding the good GFA of Cu-Zr-based alloys.

In this paper the influence of yttrium and gadolinium addition on thermal and structural behaviour of Cu-Zr bulk metallic glasses are studied.

## 2. Experimental

Pre-alloyed ingots were prepared by arc-melting of elemental Cu, Zr, Y and Gd with a purity of 99.9 wt% under an argon atmosphere to obtain the desired alloys composition. For reaching homogeneity, the samples were remelted for several times. From the Cu-Zr pre-alloys amorphous thin ribbons were prepared by means of rapid quenching from the melt using a single-roller melt-spinner under argon atmosphere. The diameter of the copper roller is 30 cm, with the quenching temperature of 1300 K and the typical rotate speed of 65 Hz.

The amorphicity and crystalline phases of the specimen were examined by X-ray diffraction (XRD). The thermal property of the melt-spin ribbon was examined by using a Netzsch DSC404 system. The ribbons were investigated by using scanning electron microscopy (SEM) with a Quanta 200 SEM (Philips FEI Company). Part of the specimen of  $\text{Cu}_{50}\text{Zr}_{25}\text{Y}_{25}$  alloy was supplied for transmission electron microscopy (TEM) observation to check the microstructures for crystallized specimen with a Tecnai F30 Analytical Microscope (Philips FEI Company).

## 3. Results and discussion

SEM images demonstrated that the microstructural evolution depends on the amount of yttrium or gadolinium, as shown in Fig. 1.

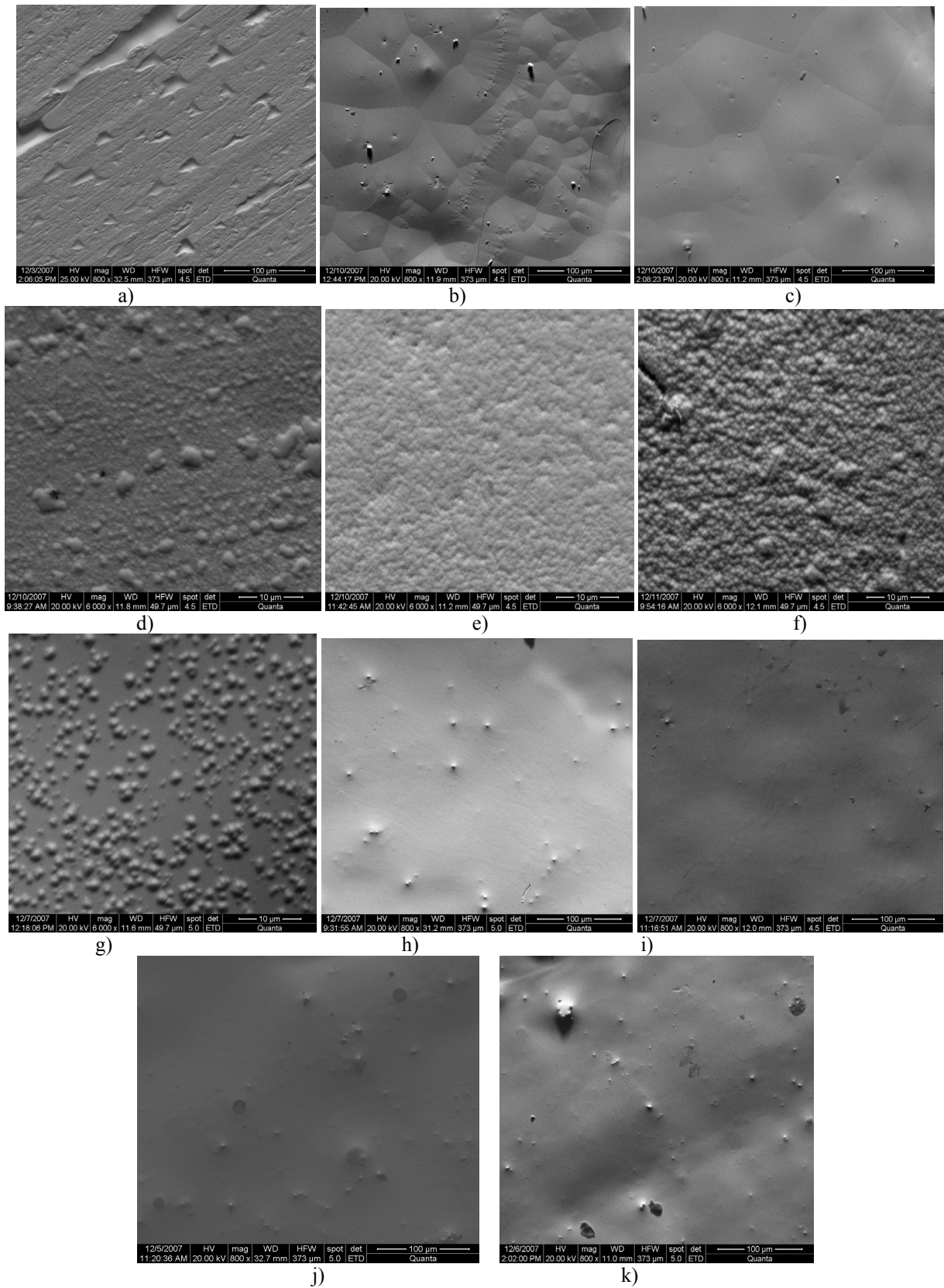


Fig. 1. SEM images of  $Cu_{50}Zr_{50-x}Me_x$  alloys; a)  $Cu_{50}Zr_{50}$  mag. 800 x, b)  $Cu_{50}Zr_{45}Y_5$  mag. 800 x, c)  $Cu_{50}Zr_{45}Gd_5$  mag. 800 x, d)  $Cu_{50}Zr_{40}Y_{10}$  mag. 6000 x, e)  $Cu_{50}Zr_{40}Gd_{10}$  mag. 6000 x, f)  $Cu_{50}Zr_{35}Y_{15}$  mag. 6000 x, g)  $Cu_{50}Zr_{35}Gd_{15}$  mag. 6000 x, h)  $Cu_{50}Zr_{30}Y_{20}$  mag. 800 x, i)  $Cu_{50}Zr_{30}Gd_{20}$  mag. 800 x, j)  $Cu_{50}Zr_{25}Y_{25}$  mag. 800 x, k)  $Cu_{50}Zr_{25}Gd_{25}$  mag. 800 x.

Recently, a newest Cu-Zr binary equilibrium phase diagram has been given by Braga et al. through experiments, as can be seen in Ref. [14], which is quite different from the currently accepted one in some composition range. However, some discrepancies still exist as yet, so the equilibrium phase diagram of Cu-Zr alloy used in this study is quoted from Ref. [15,16], as shown in Fig. 2.

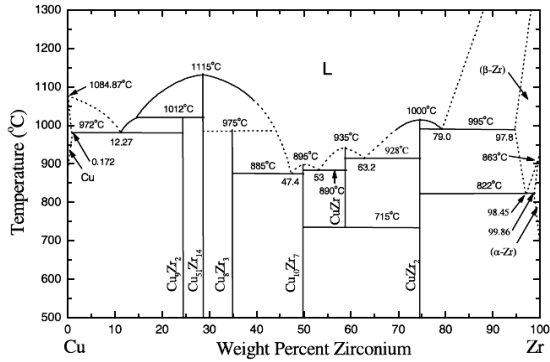


Fig. 2. The equilibrium phase diagram of Cu-Zr

Structural investigations of ribbons before DSC were carried out by X-ray diffraction (XRD) with Cu  $K_\alpha$  radiation using a Siemens D500 diffractometer. The XRD patterns of  $\text{Cu}_{50}\text{Zr}_{50}$  show the identification of following important phases:  $\text{Cu}_{10}\text{Zr}_7$ ,  $\text{CuZr}_2$  and  $\text{CuZr}$ . The X-ray diffraction patterns of the investigated alloys are presented in Fig. 3. Almost all alloys show broad diffraction maxima characteristic for an amorphous structure.

Table 1.

No	Sample	$T_{x1}$ (°C)	$T_{x2}$ (°C)
1	$\text{Cu}_{50}\text{Zr}_{45}\text{Y}_5$	425.5	
2	$\text{Cu}_{50}\text{Zr}_{40}\text{Y}_{10}$	425	
3	$\text{Cu}_{50}\text{Zr}_{35}\text{Y}_{15}$	376.6	
4	$\text{Cu}_{50}\text{Zr}_{30}\text{Y}_{20}$	284.0	359.4
5	$\text{Cu}_{50}\text{Zr}_{25}\text{Y}_{25}$	276.8	348.8
1	$\text{Cu}_{50}\text{Zr}_{45}\text{Gd}_5$	419	
2	$\text{Cu}_{50}\text{Zr}_{40}\text{Gd}_{10}$	408.6	
3	$\text{Cu}_{50}\text{Zr}_{35}\text{Gd}_{15}$	410	
4	$\text{Cu}_{50}\text{Zr}_{30}\text{Gd}_{20}$	213	352.6
5	$\text{Cu}_{50}\text{Zr}_{25}\text{Gd}_{25}$	223.5	349.2

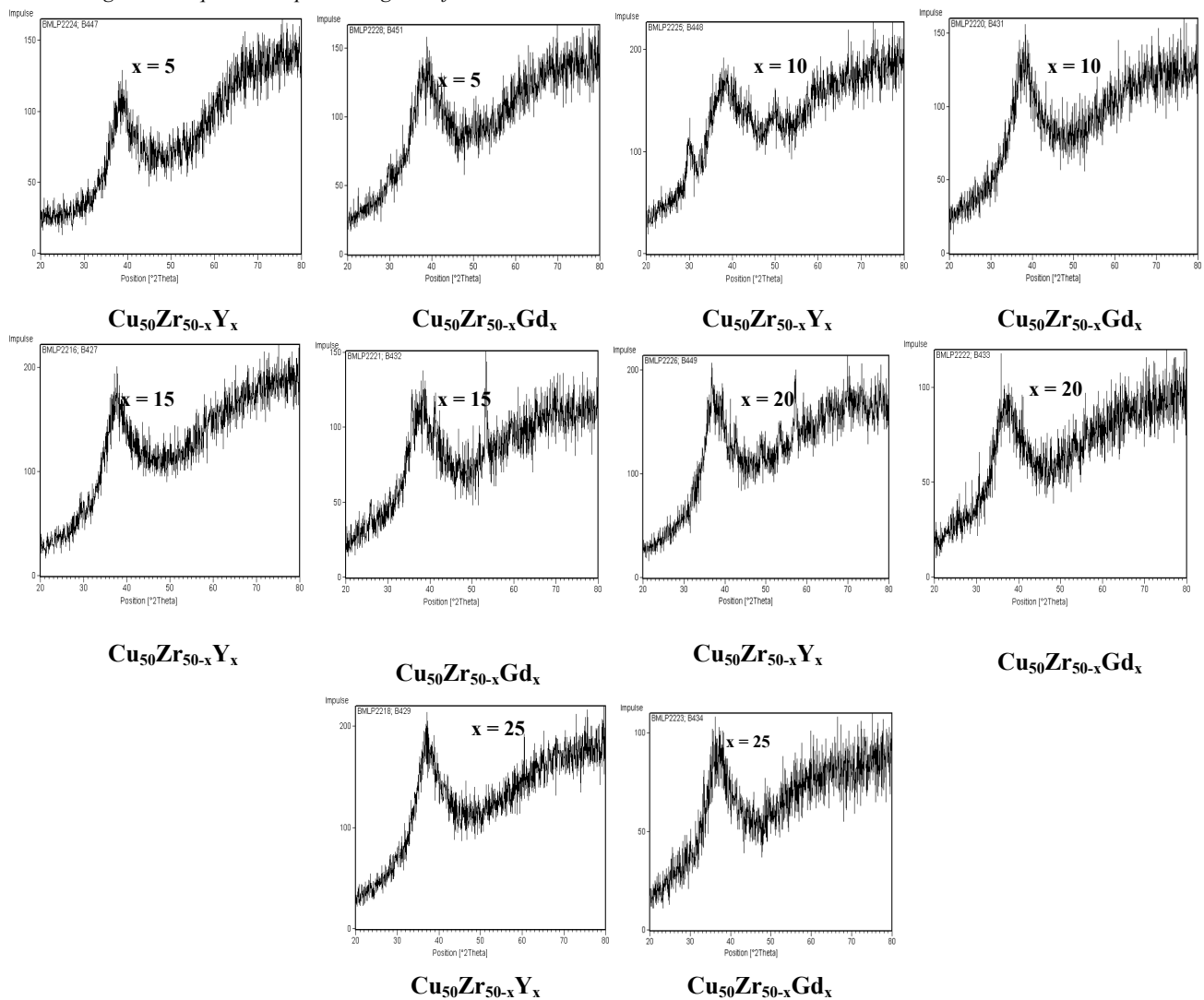


Fig. 3. X-ray diffraction patterns(Cu  $K_\alpha$  radiation) for  $\text{Cu}_{50}\text{Zr}_{50-x}\text{Me}_x$  ribbons.

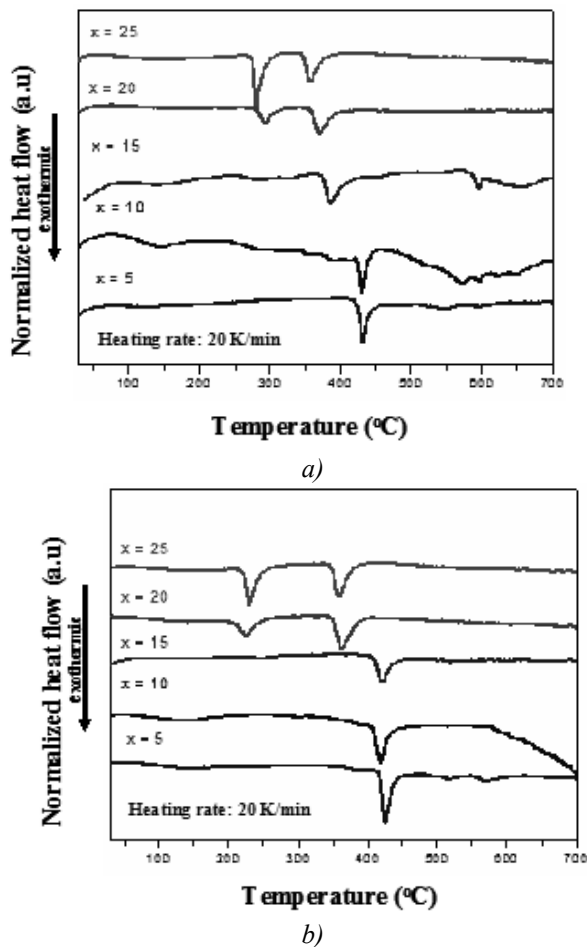


Fig. 4. DSC traces obtained at 20 K/min for a)  $\text{Cu}_{50}\text{Zr}_{50-x}\text{Y}_x$  alloys, b)  $\text{Cu}_{50}\text{Zr}_{50-x}\text{Gd}_x$  alloys.

The thermal stability of the alloys was examined with a differential scanning calorimeter (Netzsch DSC 404) under a flow of purified argon using a constant heating rate of 20 K/min. DSC trace of the  $\text{Cu}_{50}\text{Zr}_{50-x}\text{Me}_x$  (Me = Y, Gd) alloys showing a glass transition followed by crystallization.

Fig. 4 compares the crystallization behaviour of the amorphous alloys  $\text{Cu}_{50}\text{Zr}_{50-x}\text{Me}_x$  (Me = Y, Gd) by their DSC curves. The crystallization temperature of amorphous  $\text{Cu}_{50}\text{Zr}_{50}$  decreases with yttrium or gadolinium content and changes from a single step crystallization into two steps. For all alloys, the crystallization happens in well separated steps, as can be seen in DSC traces. The characteristic values of the crystallization temperatures  $T_x$  are summarized in Table 1. and in Fig. 5.

The atomic structures and the crystallization behaviour of amorphous alloys is significant to the understanding mechanism of plasticity in amorphous alloys because the activation energy for crystallization is related to the atomic arrangement of the amorphous structure. In general, the phase separation in the liquid state is believed to play an important role to the crystallization process, which in turn can affect the plastic deformation.

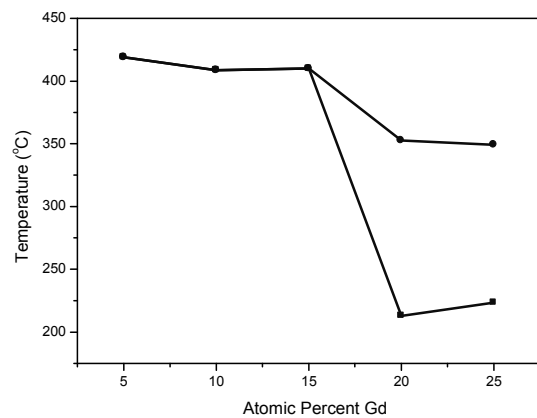
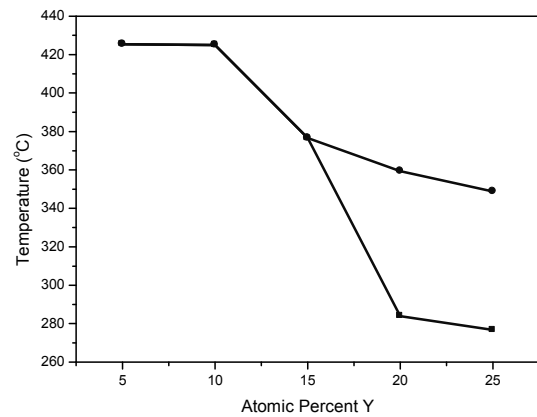


Fig. 5.  $T = f(\% \text{ at.})$  diagram for  $\text{Cu}_{50}\text{Zr}_{50-x}\text{Y}_x$  and  $\text{Cu}_{50}\text{Zr}_{50-x}\text{Gd}_x$ .

Besides, the investigation of the glassy nature of the alloys through XRD and DSC experiments, TEM studies were performed to reveal the details of structure at atomic resolution.

Fig. 6 shows the TEM image of the rapidly quenched  $\text{Cu}_{50}\text{Zr}_{25}\text{Y}_{25}$  alloy obtained with a Tecnai F30 Analytical Microscope (FEI) that proved an inhomogeneous spherical and longitudinal microstructure with a sharp interface between precipitates and matrix. Local electron diffraction and high-resolution TEM proved an amorphous structure for both regions. The contrast in the TEM image is related to local differences in chemical compositions. The nanocrystallization was confirmed by TEM analysis for  $\text{Cu}_{50}\text{Zr}_{25}\text{Y}_{25}$ . Nanoparticles are in irregular shapes (longitudinal and spherical) and have different thickness.

Fig. 7 shows the schematic diagram of crystallization process for amorphous  $\text{Cu}_{50}\text{Zr}_{50-x}\text{Me}_x$  alloys under the condition of continuous heating.

At room temperature Cu-Zr alloy matrix is fully amorphous, which can be confirmed from XRD pattern and TEM image of it. With increasing the temperature, relaxation process takes place and  $\text{CuZr}_2$  phase begins to form from the amorphous matrix due to its large negative mixture enthalpy. At this stage, no  $\text{Cu}_{10}\text{Zr}_7$  phase is detected just because an incubation time is required for it to precipitate and  $\text{CuZr}_2$  phase starts to grow. After that,  $\text{Cu}_{10}\text{Zr}_7$  phase precipitates a lot and its amount is larger than  $\text{CuZr}_2$  phase.

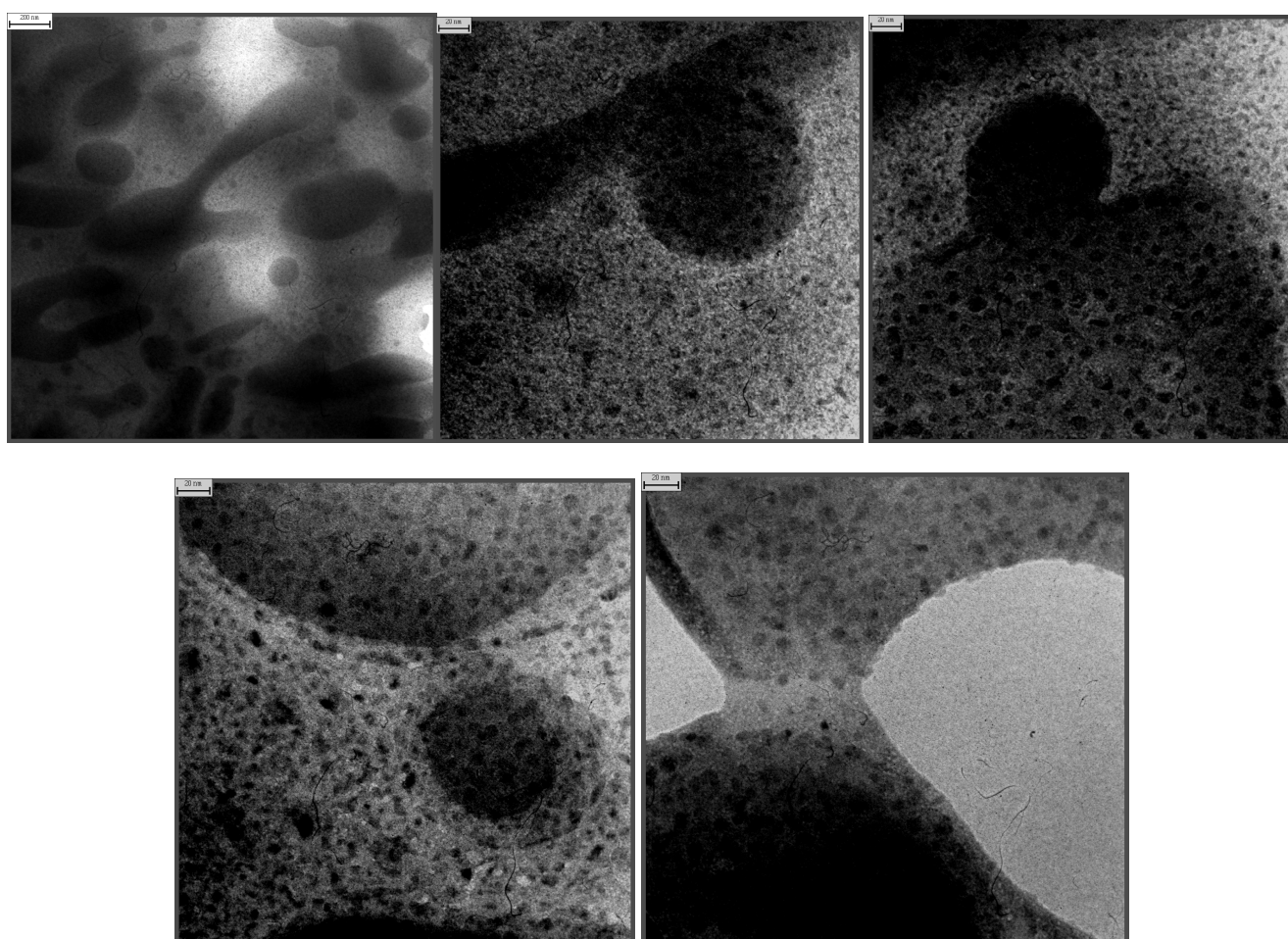


Fig. 6. TEM high resolution image of  $\text{Cu}_{50}\text{Zr}_{25}\text{Y}_{25}$ .

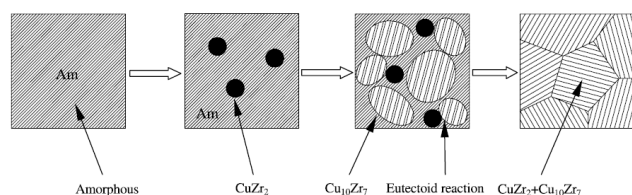


Fig. 7. Schematic diagram of crystallization process for amorphous  $\text{Cu}_{50}\text{Zr}_{50-x}\text{Me}_x$  alloys.

In the subsequent stage, a eutectoid reaction occurs, that is,  $\text{Cu}_{10}\text{Zr}_7 + \text{CuZr}_2 \leftrightarrow \text{CuZr}$  accompanying with the absorption of thermal. It is the eutectoid reaction that causes the appearance of the second endothermic peak in the DSC traces of amorphous Cu-Zr alloy.

Attributing to the good lattice matching between  $\text{Cu}_{10}\text{Zr}_7$  and  $\text{CuZr}_2$  phases and that some  $\text{Cu}_{10}\text{Zr}_7$  phases will probably take  $\text{CuZr}_2$  particles as their nuclei, which decreases the free energy of nucleation and facilitates the crystallization process. Besides, a large amount of  $\text{Cu}_{10}\text{Zr}_7$  phase is formed directly from the matrix, which retards the grain growth of  $\text{CuZr}_2$  phase. As a result, the whole matrix is occupied by  $\text{Cu}_{10}\text{Zr}_7$  phase in addition with part  $\text{CuZr}_2$

one which consists of the main final crystallization products.

As for the CuZr phase, it can be neglected because of its small amount.

In summary, the crystallization process of amorphous Cu-Zr alloy with continuous heating can be expressed as follows:

Fully amorphous  $\rightarrow \text{CuZr}_2$  particles + amorphous  $\rightarrow \text{Cu}_{10}\text{Zr}_7 + \text{CuZr}_2 \rightarrow \text{Cu}_{10}\text{Zr}_7 + \text{CuZr}_2 + \text{CuZr}$  (formed through eutectoid reaction  $\text{Cu}_{10}\text{Zr}_7 + \text{CuZr}_2 \leftrightarrow \text{CuZr}$ , but its amount is very small).

Due to the difference in chemical composition, the mean electron density varies locally, which can be detected by small-angle X-ray scattering (SAXS). The corresponding measurements will be performing at JUSIFA beam line at HASYLAB DESY Hamburg using X-ray energies.

#### 4. Conclusions

Nucleation studies of bulk metallic glasses are of importance in understanding mechanisms of phase transformation far from equilibrium, evaluating the glass-

forming ability (GFA) of the melt and producing controlled microstructure.

To extend the application of structural bulk metallic glasses, it is important to combine high glass-forming ability and good mechanical properties. In the case of Cu-based bulk amorphous alloys, recent studies have found that addition of Y and Gd to the Cu-Zr binary system reduces the melt temperature, which strongly correlates with good glass-forming ability. New Cu-based bulk amorphous alloys were formed in  $\text{Cu}_{50}\text{Zr}_{50-x}\text{Me}_x$  (Me = Y, Gd; x = 5, 10, 15, 20, 25) ternary alloys by a single roller melt spinning technique. The thermal and structural behaviour of this type of BMGs were investigated in this paper.

The addition of yttrium and gadolinium changes the thermal and crystallization behaviour of  $\text{Cu}_{50}\text{Zr}_{50}$  bulk metallic glasses. This addition greatly improves its glass-forming ability.

Cu-based BMGs have significant importance in basic research and engineering aspects.

Therefore, these types of BMGs are very promising for the further development of Cu-Zr-based alloys as engineering materials. Cu-based amorphous alloys have a potential for practical application due to their high strength and relatively low material cost.

### Acknowledgements

Special thanks are due Prof. Mariana Calin and Simon Pauly for their guidance and valuable help on each stage of the process.

The authors thank for technical assistance to: Dr. Angelika Teresiak, Andrea Ostwaldt, Birgit Opitz (XRD), Birgit Bartusch (DSC), Diana Lohse, Birgit Arnold (TEM), Alina-Mihaela Cantaragiu (SEM) and Donath Sven (Melt Spinning).

Financial support provided by European Union within the framework of the research and training networks of BMG: "Ductilisation of Bulk Metallic Glasses by Length-scale Control in BMGs Composites and Applications" (MRTN-CT-2003-504692).

### References

- [1] A. Inoue, D. Kawase, A.P. Tsai, T. Zhang, T. Masumoto, *Mater. Sci. Eng. A* **178**, 255 (1994).
- [2] L.Q. Xing, P. Ochin, J. Bigot, *J. Non-Cryst. Solids* **205–207**, 637 (1996).
- [3] U. Koster, J. Meinhardt, R. Roos, H. Liebertz, *Appl. Phys. Lett.* **69**, 664 (1996).
- [4] B.S. Murty, D.H. Ping, K. Hono, A. Inoue, *Acta Mater.* **48**, 3985 (2000).
- [5] A. Inoue, T. Zhang, N. Nishiyama, K. Ohba, T. Masumoto, *Mater. Trans. JIM* **34**, 1234 (1993).
- [6] S.H. Zhou, J. Schmid, F. Sommer, *Thermochim. Acta* **339**, 1 (1999).
- [7] U. Koster, J. Meinhardt, S. Roos, R. Busch, *Mater. Sci. Eng. A* **226–228**, 995 (1997).
- [8] C.F. Li, J. Saida, A. Inoue, *Mater. Trans. JIM* **41**, 1521 (2000).
- [9] L.Q. Xing, P. Ochin, *Acta Mater.* **45**, 3765 (1997).
- [10] M.W. Chen, T. Zhang, A. Inoue, A. Sakai, T. Sakurai, *Appl. Phys. Lett.* **75**, 1697 (1999).
- [11] A. Inoue, T. Zhang, J. Saida, M. Matsubara, M.W. Chen, T. Sakurai, *Mater. Trans. JIM* **40**, 1137 (1999).
- [12] A. Inoue, T. Zhang, J. Saida, M. Matsubara, M.W. Chen, T. Sakurai, *Mater. Trans. JIM* **40**, 3381 (1999).
- [13] A. Inoue, T. Zhang, M.W. Chen, T. Sakurai, *Mater. Trans. JIM* **40**, 1382 (1999).
- [14] M.H. Braga, L.F. Malheiros, F. Castro, D. Soares, *Z. Metallkd.* **89**, 541 (1998).
- [15] P. Villars, L.D. Calvert, in: *Pearson's Handbook of Crystallographic Data for Intermetallic Phase*, Materials Park Press, 1511 (1991).
- [16] K.J. Zeng, M. Hämmäläinen, H.L. Lukas: Phase diagram of Cu-Zr alloys, *J. Phase Equilibria* **15**, 577 (1994).

\*Corresponding author: vis13\_2000@yahoo.com